

CrossMark
click for updatesCite this: *RSC Adv.*, 2015, 5, 29878

Mechanochromism and aggregation induced emission in benzothiazole substituted tetraphenylethylenes: a structure function correlation†

Thaksen Jadhav, Bhausheb Dhokale, Shaikh M. Mobin and Rajneesh Misra*

The donor–acceptor benzothiazole substituted tetraphenylethylenes (BT-TPEs) **3a–3c** were designed and synthesized to examine the effect of the linkage between the BT and the TPE unit on the photophysical, aggregation induced emission (AIE) and mechanochromic properties. The syntheses of BT-TPEs **3a–3c** were achieved by the Pd-catalyzed Suzuki cross-coupling reaction of bromobenzothiazoles **1a–1c** with 4-(1,2,2-triphenylvinyl)phenylboronic acid pinacol ester (**2**). The study showed that their photophysical, AIE and mechanochromic properties are dependent on the linkage between the BT and the TPE unit (*ortho*, *meta*, and *para*). The *meta* isomer **3b** shows the highest grinding induced spectral shift (51 nm) whereas the *ortho* isomer **3a** shows the lowest grinding induced spectral shift (9 nm). The single crystal X-ray structures reveal the highly twisted conformation and tight packing in BT-TPE **3a** compared to **3b**. The thermogravimetric analysis of BT-TPEs shows good thermal stability. The computational study reveals the donor–acceptor nature of the BT-TPEs. The structure–function correlation indicates that the mechanochromic and aggregation induced emission (AIE) properties were dependent on the linkage between BT and TPE.

Received 19th March 2015
Accepted 23rd March 2015

DOI: 10.1039/c5ra04881h

www.rsc.org/advances

Introduction

The research on small organic molecules, showing response to environmental stimuli in the solid state has gained momentum due to their applications in sensors, displays, fluorescent probes and information storage devices.¹ Mechanochromism is the response of a material toward mechanical strain, which causes changes in their absorption or emission properties.² The literature reveals there is a lack of systematic study, to understand the exact mechanism and principle of mechanochromism. The effect of end groups, alkyl chain length, their position, hydrogen bonding and strength of donor–acceptor interaction in different fluorophores on mechanochromism have been explored.^{3–6} The mode of molecular packing in the crystal structure, variation in the planarity, phase transition between crystalline phase to amorphous phase are the major factors that govern the mechanochromism.^{3–6}

The benzothiazole (BT) is weak electron acceptor and has been used in donor–acceptor systems for various optoelectronic

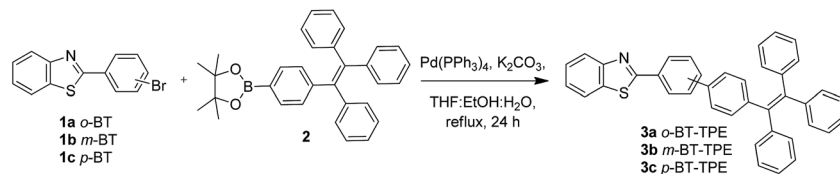
applications.⁷ On the other hand the propeller shaped tetraphenylethylene (TPE) is weak electron donor and exhibits aggregation induced emission (AIE).⁸ Recently BT substituted TPEs were reported for their mechanochromic behavior.⁹ Our group was interested to explore the effect of linkage between TPE and BT unit on the donor–acceptor strength, AIE, and mechanochromic property of BT-TPE isomers. We have designed and synthesized three donor–acceptor isomers (*ortho*, *meta*, and *para*) BT-TPE **3a–3c** and explored their photophysical and mechanochromic properties.

Result and discussion

The syntheses of BT-TPEs **3a–3c** are shown in Scheme 1. The bromo-benzothiazoles **1a–1c** were synthesized by the condensation reaction of 2-amino thiophenol and (*ortho/meta/para*)-bromobenzaldehyde respectively in the presence of ammonium chloride and acetic acid.¹⁰ The Suzuki cross-coupling reaction of benzothiazoles **1a–1c** with 4-(1,2,2-triphenylvinyl)phenylboronic acid pinacol ester (**2**) using Pd(PPh₃)₄ as a catalyst resulted **3a–3c** in 67%, 78% and 66% yields respectively. The purification of the BT-TPEs **3a–3c** was achieved by column chromatography. All the BT-TPEs **3a–3c** were well characterized by ¹H, ¹³C NMR and HRMS techniques. The BT-TPEs **3a**, and **3b** were also characterized by single-crystal X-ray diffraction technique.

Indian Institute of Technology Indore, Discipline of Chemistry, Chemistry, Indore, India. E-mail: rajneeshmisra@iiti.ac.in

† Electronic supplementary information (ESI) available: Experimental procedures, NMR spectra, UV-vis spectra, mechanochromic effect, computational data and crystal structural data for **3a** and **3b**. CCDC 1044876 and 1044877. For ESI and crystallographic data in CIF or other electronic format see DOI: 10.1039/c5ra04881h



Scheme 1 Synthesis of BT-TPEs 3a–3c.

The thermal stability of the BT-TPEs 3a–3c was investigated by the thermogravimetric analysis (TGA) at heating rate of 10 °C min⁻¹, under nitrogen atmosphere (Fig. S3†). The BT-TPEs 3a and 3b show the decomposition temperature at 349 °C, and 3c at 361 °C for 5% weight loss.

The electronic absorption spectra of the BT-TPEs 3a–3c are shown in Fig. S4,† and the data are summarized in Table S2.† The BT-TPEs 3a–3c exhibit absorption band between 250–400 nm with extinction coefficient between 34 000–55 000 L M⁻¹ cm⁻¹. The BT-TPEs 3b and 3c exhibits 14 nm, and 46 nm red shifted absorption compared to the TPE unit (299 nm). On the other hand 3a show similar absorption behavior like TPE.¹¹ The red shift in the absorption spectra follows the order 3c > 3b > 3a, which reveals that 3c exhibits stronger electronic communication compared to 3a and 3b. The trend further suggests that 3a has more twisted structure and large dihedral angle between the BT and TPE unit, which is evident from the single crystal X-ray structure and computational studies. The BT-TPEs 3a–3c are

weakly fluorescent in solution, due to free molecular rotations of tetraphenylethylene unit in solution resulting in nonradiative decay of excited state.¹²

The AIE property of BT-TPEs 3a–3c were studied by absorption and fluorescence spectroscopy in THF–water mixtures with different water fraction. The BT-TPEs 3a–3c are highly soluble in tetrahydrofuran (THF) and insoluble in water, by increasing the water fraction in the THF–water mixture, it transforms into aggregated particles, resulting change in the absorption and fluorescence behavior. The BT-TPEs 3a–3c show different AIE behavior (Fig. 1). The quantitative estimation of the AIE process was obtained by calculating the fluorescence quantum yields for 3a–3c in the mixtures of water and THF in various proportions, using 9,10-diphenylanthracene as standard. In pure THF solution the BT-TPEs exhibit poor fluorescence quantum yield, which remains constant until the molecules start aggregating significantly (AIE effect).

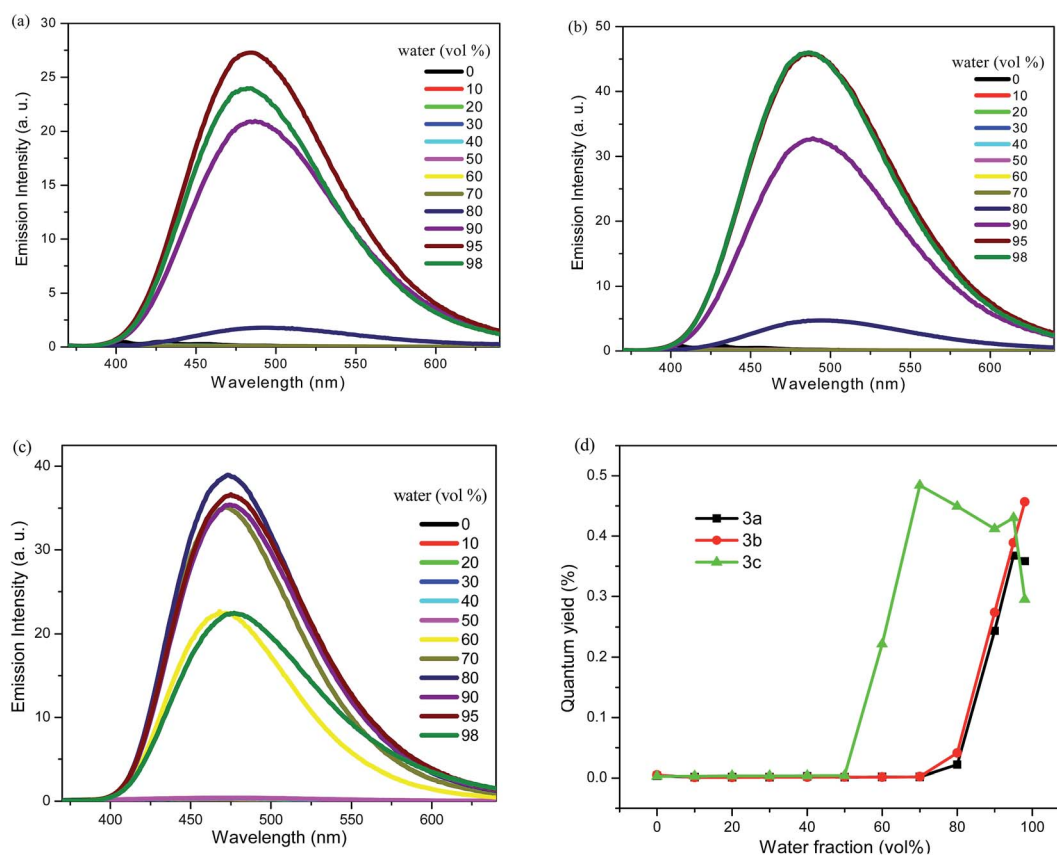


Fig. 1 Fluorescence spectra of (a) 3a, (b) 3b and (c) 3c in THF–water mixtures with different water fractions (10 μM). (d) Fluorescence quantum yields of the BT-TPEs in water–THF mixtures against different volume fractions of water.

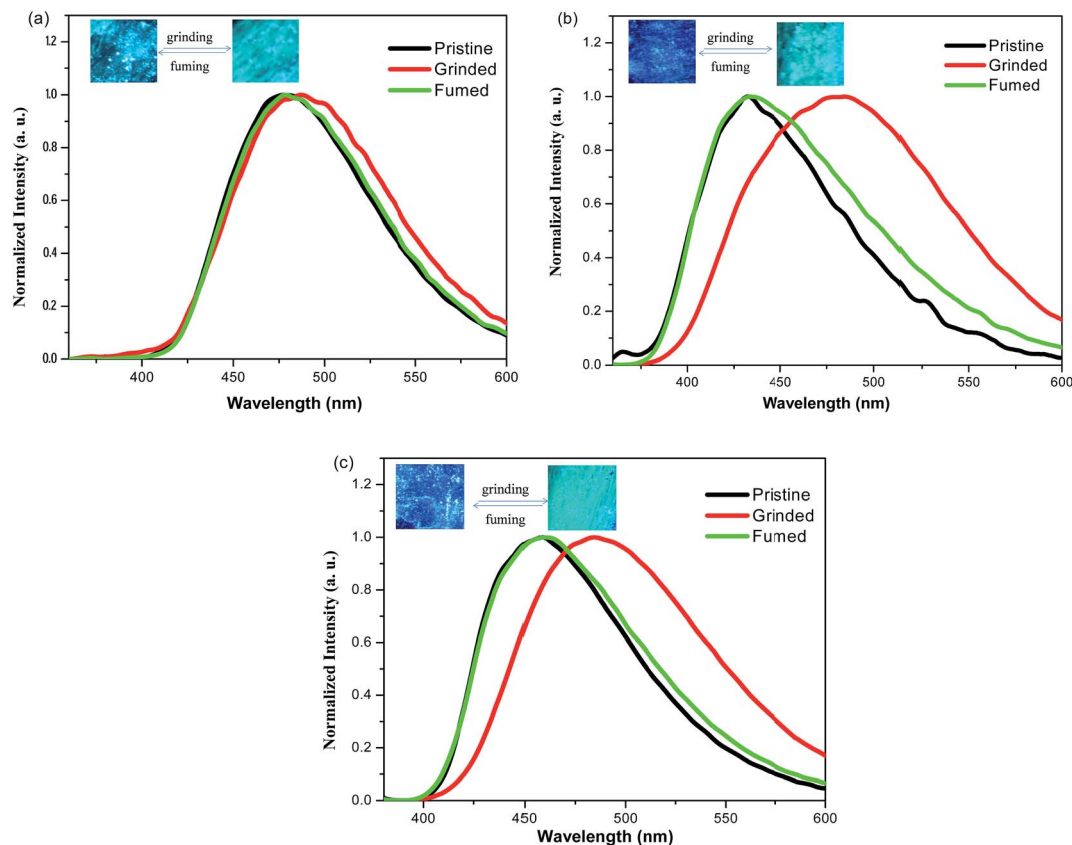


Fig. 2 Emission spectra of (a) **3a**, (b) **3b** and (c) **3c** as pristine, grinded and fumed solids.

Table 1 Emission wavelengths of **3a–3c** under various external stimuli

BT-TPEs	$\lambda_{\text{Pristine}}$ (nm)	λ_{Grinded} (nm)	λ_{Fumed} (nm)	$\Delta\lambda$ (nm) ^a
3a	478	487	478	9
3b	432	483	439	51
3c	458	484	460	26

^a Grinding-induced spectral shift, $\Delta\lambda = \lambda_{\text{Grinded}} - \lambda_{\text{Pristine}}$.

It was observed that different percentage of water fraction was required for **3a–3c** to exhibit AIE. The BT-TPEs **3a** and **3b** require more than 80% water fraction, whereas **3c** requires more than 50% water fraction (Fig. 1). The **3a** in pure THF solution shows fluorescence quantum yield 0.004, which was increased to 0.368 at 95% water fraction and then slightly decreased to 0.359 at 98% water fraction. The **3b**, in pure THF solution shows fluorescence quantum yield 0.005, which was increased to 0.457 at 95% water fraction. In case of **3c**, pure THF solution shows fluorescence quantum yield 0.003, which was increased to 0.484 at 70% water fraction and remains almost constant up to 95% water fraction, and then decreased to 0.295 at 98% water fraction. The images of BT-TPEs **3a–3c** in THF–water mixture with different water fractions under UV illumination are shown in Fig. S6,[†] which clearly show different AIE behavior, and can be attributed to the formation of various

aggregate states of the molecules in the THF–water mixture. The AIE behavior was further explored by studying the absorption spectra in the THF–water mixtures (10 mM) (Fig. S5[†]). The absorption spectra of **3a**, and **3b** at 80% water fraction, whereas **3c** at 60% water fraction started to show light scattering or Mie effect of the nanoaggregate suspension in the THF–water mixtures.¹³

The mechanochromic properties of BT-TPEs **3a–3c** were studied by solid state emission spectroscopy. The emission spectra of **3a–3c** are shown in Fig. 2 and the corresponding data are summarized in Table 1. The study reveals that mechanochromism was found to be dependent on the position of TPE unit with respect to the BT unit. The BT-TPEs **3a–3c** in pristine form emit at 478 nm, 432 nm, and 458 nm, which on grinding with mortar and pestle show red shifted emission at 487 nm, 483 nm, and 484 nm respectively. The BT-TPEs **3a–3c** show grinding induced spectral shift ($\Delta\lambda$) of 9 nm, 51 nm, and 26 nm respectively. In pristine form, the isomers **3a–3c** show different emission behavior and follows the trend as **3a** > **3c** > **3b**, which is same as the trend in spectral shift ($\Delta\lambda$). The grinded BT-TPEs **3a–3c** emit in the similar region. The spectral changes induced by grinding can be restored by solvent fuming. This mechanochromic conversion can be repeated by repeated grinding and fuming processes as these processes do not cause any chemical change (Fig. S7–S9, ESI[†]).

The solid state absorption spectra (Fig. 3) of **3a–3c** were recorded to understand the emission behavior and D–A

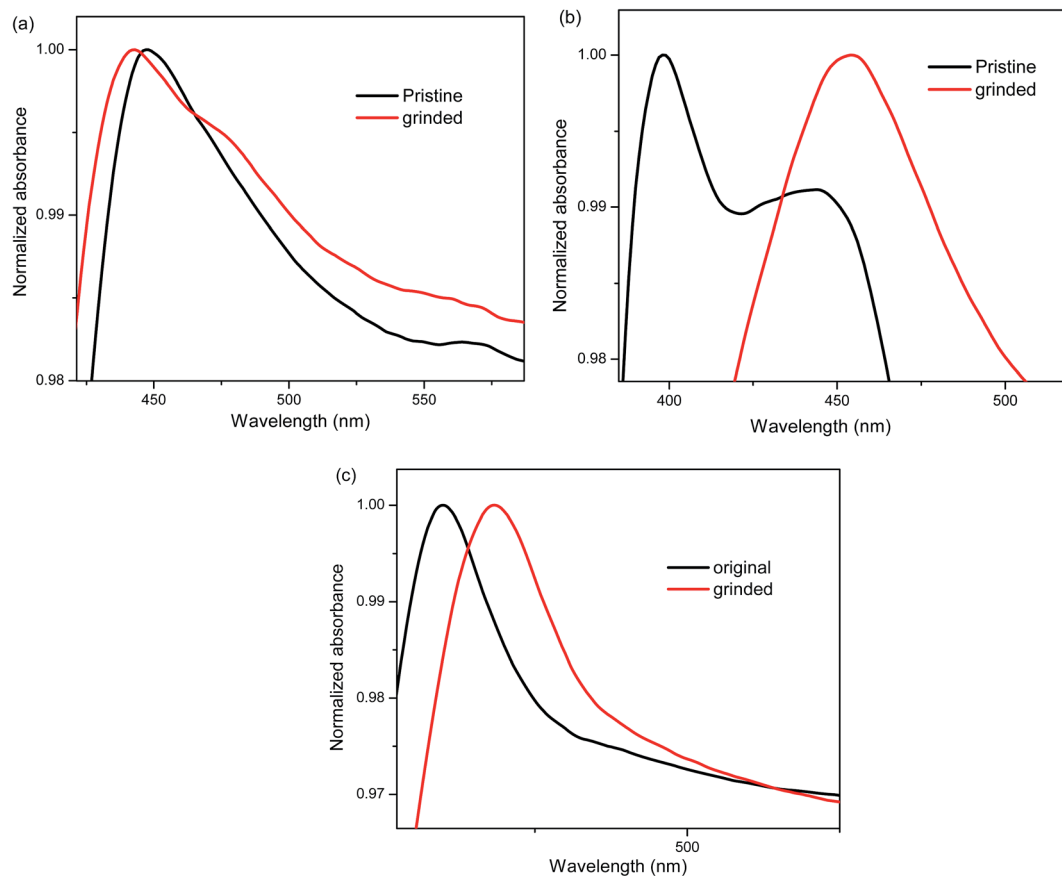


Fig. 3 Solid state absorption spectra of (a) **3a**, (b) **3b** and (c) **3c** in crystalline and its grinded form.

interaction in solid state under various external stimuli, the data are summarized in Table S3.† The BT-TPE **3a** show similar absorption behavior in pristine and grinded form with blue shift of 4 nm, and broadening of the shoulder at 471 nm. In case of **3b**, pristine form shows two peaks at 398, and 444 nm, and after grinding only one band at 455 nm was observed. The pristine sample of **3c** absorbs at 420 nm, which on grinding shifted to 436 nm. The grinding induced red shift in solid state absorption spectra indicates planarization and enhanced conjugation.

The powder X-ray diffractions (PXRD) of pristine, grinded and fumed forms of BT-TPEs **3a–3c** (Fig. 4) were studied. The diffraction patterns for pristine samples show sharp peaks, which is characteristic property of the crystalline samples. The pristine samples upon grinding show broad diffuse bands indicating amorphous nature. The grinded samples after fuming with dichloromethane restore the sharp peaks, suggesting regeneration of the crystalline nature. The PXRD study reveals that the morphological change from the crystalline state

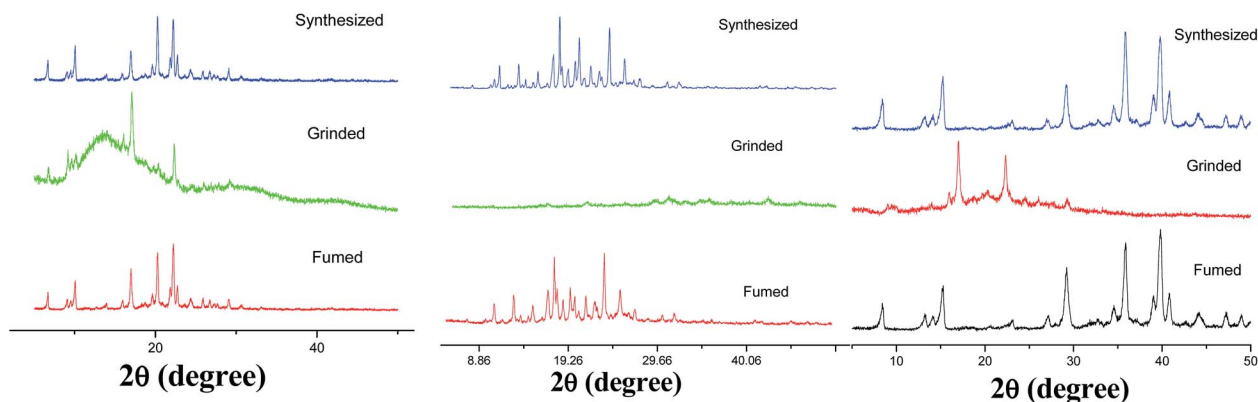


Fig. 4 PXRD curves of **3a**(a), **3b**(b) and **3c**(c) in synthesized, grinded and fumed form.

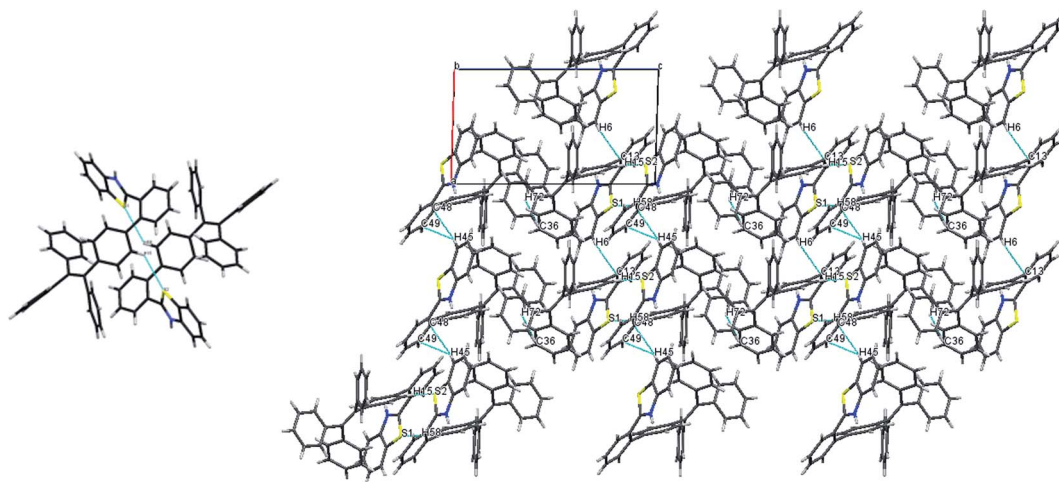


Fig. 5 Crystal structure and packing diagram of **3a**.

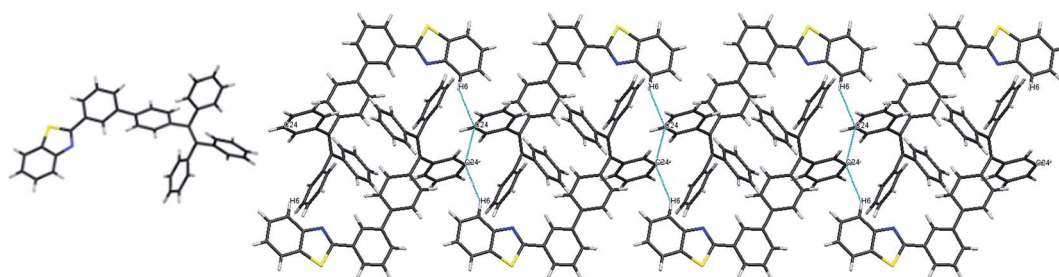


Fig. 6 Crystal structure and packing diagram of **3b**.

to the amorphous state and *vice versa* is associated with the mechanochromism in BT-TPEs **3a–3c**.

The photophysical behaviors of BT-TPEs **3a–3c** were correlated with solid state packing by analyzing the single crystals of **3a** and **3b** (details are provided in Table S1, ESI†). Fig. 5 and 6

depict the molecular structures which show highly twisted conformations. In the crystal structure of **3a**, two molecules exist in an asymmetric unit. The two molecules are held together *via* two mutual C(15)–H(15)⋯S(2) (2.942 Å) and C(58)–H(58)⋯S(1) (2.956 Å) interactions. The torsional angles

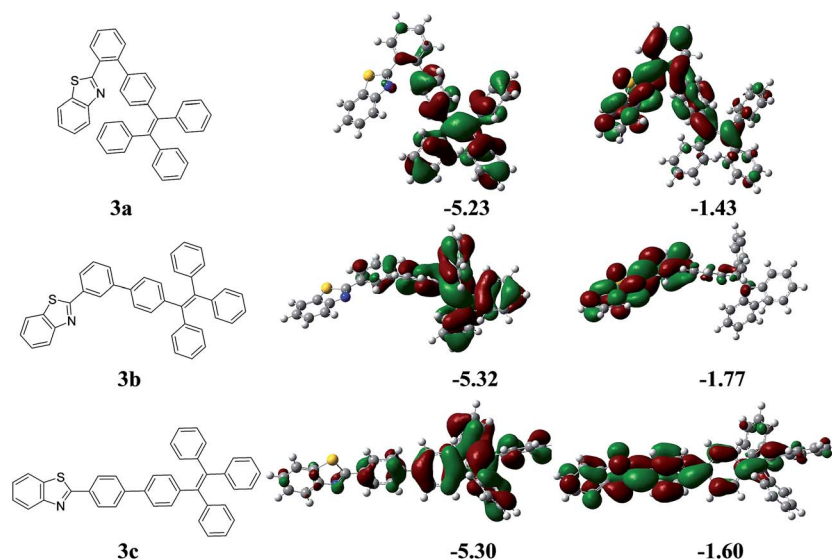


Fig. 7 HOMO and LUMO frontier molecular orbitals of **3a–3c** at the B3LYP/6-31G(d) level.

between the benzothiazole unit and phenyl ring are 4° and 53° for **3a** and **3b** respectively. Further, the torsional angles between the phenyl attached to benzothiazole unit and TPE phenyl are 32° and 43° for **3a** and **3b** respectively. This reveals that **3a** has highly twisted conformation than the **3b**.

The packing diagram of **3a** show extensive supramolecular interactions. The two molecule in an asymmetric unit forms dimer, which extends into the sheet like structural framework along *a*-axis *via* interactions C(45)–H(45)⋯π(C45–C52) (2.779 Å), C(72)–H(72)⋯π(C34–C39) (3.868 Å) and C(6)–H(6)⋯π(C8–C13) (2.837 Å). This sheet further extends into the complex 3-D structural framework *via* interaction C(4)–H(4)⋯π(C22–C27) (3.434 Å) (Fig. 5). The supramolecular packing of **3b** is shown in the Fig. 6, in which a rod like framework was formed *via* mutual C(6)–H(6)⋯π(C24) (2.853 Å) interactions and weak π⋯π staking interaction between C(24)⋯C(24) (3.360 Å). The packing diagram reveals tight packing in **3a** than **3b**.

The geometry and electronic structure of **3a–3c** were investigated by density functional theory (DFT) calculations using the Gaussian 09W program. The DFT calculations were performed at the B3LYP/6-31G(d) level of theory.¹⁴ The optimized structures for **3a–3c** show twisted conformation (Fig. 7). The highest occupied molecular orbitals (HOMOs) of **3a–3c** are majorly distributed on the TPE unit, whereas lowest unoccupied molecular orbitals (LUMOs) are located on the benzothiazole unit, indicating the donor–acceptor behavior (Fig. 7).

Conclusion

In conclusion we have designed, and synthesized three donor–acceptor BT-TPEs **3a–3c** by the Pd-catalyzed Suzuki coupling reaction. Their structural, photophysical, aggregation induced emission (AIE) and mechanochromic properties were found to be the function of the linkage between the TPE and the BT units. The variation in the D–A interaction, molecular structure and solid-state packing perturb the mechanochromic behavior of BT-TPEs **3a–3c**. The results represent the structure function correlation on mechanochromism and will be helpful in the development of mechano sensors.

Experimental details

General methods

Chemicals were used as received unless otherwise indicated. All oxygen or moisture sensitive reactions were performed under nitrogen/argon atmosphere. ¹H NMR (400 MHz), and ¹³C NMR (100 MHz) spectra were recorded on the Bruker Avance (III) 400 MHz instrument by using CDCl₃. ¹H NMR chemical shifts are reported in parts per million (ppm) relative to the solvent residual peak (CDCl₃, 7.26 ppm). Multiplicities are given as: s (singlet), d (doublet), t (triplet), q (quartet), dd (doublet of doublets), dt (doublet of triplets), m (multiplet), and the coupling constants, *J*, are given in Hz. ¹³C NMR chemical shifts are reported relative to the solvent residual peak (CDCl₃, 77.36 ppm). Thermogravimetric analyses were performed on the Mettler Toledo Thermal Analysis system. UV-visible absorption spectra were recorded on a Carry-100 Bio UV-visible

Spectrophotometer. Emission spectra were taken in a fluoromax-4p fluorimeter from HoribaYovin (model: FM-100). The excitation and emission slits were 2/2 nm for the emission measurements. All of the measurements were done at 25 °C. HRMS was recorded on Bruker-Daltonics, micrOTOF-Q II mass spectrometer. The density functional theory (DFT) calculation were carried out at the B3LYP/6-31G(d) level in the Gaussian 09 program. TD-DFT calculations was performed at the B3LYP/6-31G(d) level in dichloromethane solvent using IEFPCM formulation for solvent effect.

Synthesis and characterization of **3a–3c**

3a. Pd(PPh₃)₄ (0.004 mmol) was added to a well degassed solution of 2-(2-bromophenyl)-1*H*-benzo[*d*]imidazole (**2a**) (0.4 mmol), **5** (0.48 mmol), K₂CO₃ (1.2 mmol) in a mixture of toluene (12 mL)/ethanol (4.0 mL)/H₂O (1.0 mL). The resulting mixture was stirred at 80 °C for 24 h under argon atmosphere. After cooling, the mixture was evaporated to dryness and the residue subjected to column chromatography on silica to yield the desired product **3a** as colorless powder. The compound was recrystallized from DCM : ethanol (8 : 2) mixtures. Yield: 67.0%. ¹H NMR (400 MHz, CDCl₃, 25 °C): δ 8.01–8.07 (m, 2H), 7.83 (d, 1H, *J* = 8 Hz), 7.46–7.51 (m, 3H), 7.38–7.45 (m, 2H), 6.99–7.12 (m, 19H) ppm; ¹³C NMR (100 MHz, CDCl₃, 25 °C): δ 167.8, 152.8, 143.6, 143.5, 143.5, 143.3, 141.5, 141.2, 140.4, 138.1, 136.7, 132.7, 131.4, 131.3, 131.3, 130.7, 130.4, 129.9, 129.4, 127.6, 126.5, 125.9, 124.9, 123.3, 121.1, 0.00 ppm; HRMS (ESI): calcd for C₃₉H₂₇NS: 542.1937 (M + H)⁺, found 542.1947.

3b. Pd(PPh₃)₄ (0.004 mmol) was added to a well degassed solution of 2-(3-bromophenyl)-1*H*-benzo[*d*]imidazole (**2b**) (0.4 mmol), **5** (0.48 mmol), K₂CO₃ (1.2 mmol) in a mixture of toluene (12 mL)/ethanol (4.0 mL)/H₂O (1.0 mL). The resulting mixture was stirred at 80 °C for 24 h under argon atmosphere. After cooling, the mixture was evaporated to dryness and the residue subjected to column chromatography on silica to yield the desired product **3b** as colorless powder. The compound was recrystallized from DCM : ethanol (8 : 2) mixtures. Yield: 78.0%. ¹H NMR (400 MHz, CDCl₃, 25 °C): δ 8.29 (t, 1H, *J* = 1.6 Hz), 8.09 (d, 1H, *J* = 8 Hz), 8.00–8.02 (m, 1H), 7.92 (d, 1H, *J* = 8 Hz), 7.66–7.69 (m, 1H), 7.49–7.54 (m, 2H), 7.38–7.46 (m, 3H), 7.04–7.17 (m, 17H) ppm; ¹³C NMR (100 MHz, CDCl₃, 25 °C): δ 168.4, 154.5, 144.03, 143.99, 143.7, 142.0, 141.7, 140.7, 138.2, 135.4, 134.4, 132.2, 131.74, 131.68, 129.8, 129.7, 128.2, 128.1, 128.0, 126.93, 126.86, 126.81, 126.73, 126.7, 126.2, 125.6, 123.6, 122.0, 0.00 ppm; HRMS (ESI): calcd for C₃₉H₂₇NS: 542.1937 (M + H)⁺, found 542.1942.

3c. Pd(PPh₃)₄ (0.004 mmol) was added to a well degassed solution of 2-(4-bromophenyl)-1*H*-benzo[*d*]imidazole (**2c**) (0.4 mmol), **5** (0.48 mmol), K₂CO₃ (1.2 mmol) in a mixture of toluene (12 mL)/ethanol (4.0 mL)/H₂O (1.0 mL). The resulting mixture was stirred at 80 °C for 24 h under argon atmosphere. After cooling, the mixture was evaporated to dryness and the residue subjected to column chromatography on silica to yield the desired product **3c** as colorless powder. The compound was recrystallized from DCM : ethanol (8 : 2) mixtures. Yield: 66.0%. ¹H NMR (400 MHz, CDCl₃, 25 °C): δ 8.12 (d, 2H, *J* = 12 Hz), 8.08

(d, 1H, $J = 8$ Hz), 7.91 (d, 1H, $J = 4$ Hz), 7.68 (d, 2H, $J = 12$ Hz), 7.48–7.52 (m, 1H), 7.37–7.43 (m, 3H), 7.03–7.16 (m, 17H) ppm; ^{13}C NMR (100 MHz, CDCl_3 , 25 °C): δ 168.1, 154.5, 144.0, 143.96, 143.95, 143.92, 143.51, 141.74, 140.6, 138.0, 135.4, 132.6, 132.3, 131.7, 131.68, 131.67, 128.2, 128.15, 128.07, 127.99, 127.7, 126.94, 126.89, 126.83, 126.7, 126.5, 125.5, 123.5, 122.0, 0.00 ppm; HRMS (ESI): calcd for $\text{C}_{39}\text{H}_{27}\text{NS}$: 542.1937 ($\text{M} + \text{H}$) $^+$, found 542.1938.

Acknowledgements

We acknowledge the support by DST, and CSIR Govt. of India, New Delhi. T J thanks UGC, B D thanks to CSIR New Delhi for their fellowships. We acknowledge Sophisticated Instrumentation Centre (SIC) facility, IIT Indore.

References

- (a) Y. Sagara and T. Kato, *Nat. Chem.*, 2009, **1**, 605; (b) D. A. Davis, A. Hamilton, J. L. Yang, L. D. Cremer, D. Van Gough, S. L. Potisek, M. T. Ong, P. V. Braun, T. J. Martinez, S. R. White, J. S. Moore and N. R. Sottos, *Nature*, 2009, **459**, 68; (c) Y. J. Dong, B. Xu, J. B. Zhang, X. Tan, L. J. Wang, J. L. Chen, H. G. Lv, S. P. Wen, B. Li, L. Ye, B. Zou and W. J. Tian, *Angew. Chem., Int. Ed.*, 2012, **51**, 10782; (d) X. L. Luo, J. N. Li, C. H. Li, L. P. Heng, Y. Q. Dong, Z. P. Liu, Z. S. Bo and B. Z. Tang, *Adv. Mater.*, 2011, **23**, 3261; (e) Q. A. Best, N. Sattenapally, D. J. Dyer, C. N. Scott and M. E. McCarroll, *J. Am. Chem. Soc.*, 2013, **135**, 13365.
- (a) Z. Chi, X. Zhang, B. Xu, X. Zhou, C. Ma, Y. Zhang, S. Liu and J. Xu, *Chem. Soc. Rev.*, 2012, **41**, 3878; (b) A. Pucci and G. Ruggeri, *J. Mater. Chem.*, 2011, **21**, 8282; (c) M. M. Caruso, D. A. Davis, Q. Shen, S. A. Odom, N. R. Sottos, S. R. White and J. S. Moore, *Chem. Rev.*, 2009, **109**, 5755; (d) K. Ariga, T. Mori and J. P. Hill, *Adv. Mater.*, 2012, **24**, 158.
- L. Bu, M. Sun, D. Zhang, W. Liu, Y. Wang, M. Zheng, S. Xue and W. Yang, *J. Mater. Chem. C*, 2013, **1**, 2028.
- (a) X. Zhang, Z. Chi, B. Xu, L. Jiang, X. Zhou, Y. Zhang, S. Liu and J. Xu, *Chem. Commun.*, 2012, **48**, 10895; (b) S. Xue, W. Liu, X. Qiu, Y. Gao and W. Yang, *J. Phys. Chem. C*, 2014, **118**, 18668.
- (a) M. Sase, S. Yamaguchi, Y. Sagara, I. Yoshikawa, T. Mutai and K. Araki, *J. Mater. Chem.*, 2011, **21**, 8347; (b) J. Kunzleman, M. Kinami, B. Crenshaw, J. Protasiewicz and C. Weder, *Adv. Mater.*, 2008, **20**, 119; (c) N. Nguyen, G. Zhang, J. Lu, A. Sherman and C. Fraser, *J. Mater. Chem.*, 2011, **21**, 8409; (d) Y. Sagara, T. Mutai, I. Yoshikawa and K. Araki, *J. Am. Chem. Soc.*, 2007, **129**, 1520; (e) T. Han, Y. Zhang, X. Feng, Z. Lin, B. Tong, J. Shi, J. Zhi and Y. Dong, *Chem. Commun.*, 2013, **49**, 7049; (f) Y. Zhang, T. Han, S. Gu, T. Zhou, C. Zhao, Y. Guo, X. Feng, B. Tong, J. Bing, J. Shi, J. Zhi and Y. Dong, *Chem.–Eur. J.*, 2014, **20**, 8856.
- (a) R. Davis, N. Kumar, S. Abraham, C. Suresh, N. Rath, N. Tamaoki and S. Das, *J. Phys. Chem. C*, 2008, **112**, 2137; (b) N. Kumar, S. Varghese, N. Rath and S. Das, *J. Phys. Chem. C*, 2008, **112**, 8429; (c) N. Kumar, S. Varghese, C. Suresh, N. Rath and S. Das, *J. Phys. Chem. C*, 2009, **113**, 11927; (d) R. Thomas, S. Varghese and G. Kulkarni, *J. Mater. Chem.*, 2009, **19**, 4401; (e) Q. Liu, W. Liu, B. Yao, H. Tian, Z. Xie, Y. Geng and F. Wang, *Macromolecules*, 2007, **40**, 1851; (f) P. Gautam, R. Maragani, S. M. Mobin and R. Misra, *RSC Adv.*, 2014, **4**, 52526.
- (a) V. Hrobarikova, P. Hrobarik, P. Gajdos, I. Fitisil, M. Fakis, P. Persephonis and P. Zahradnik, *J. Org. Chem.*, 2010, **75**, 3053; (b) P. Hrobarik, V. Hrobarikova, I. Sigmundov, P. Zahradnik, M. Fakis, I. Polyzos and P. Persephonis, *J. Org. Chem.*, 2011, **76**, 8726; (c) P. Gautam, R. Maragani and R. Misra, *Tetrahedron Lett.*, 2014, **55**, 6827.
- (a) W. Z. Yuan, P. Lu, S. Chen, J. W. Y. Lam, Z. Wang, Y. Liu, H. S. Kwok, Y. Ma and B. Z. Tang, *Adv. Mater.*, 2010, **22**, 2159; (b) B. Xu, Z. Chi, H. Li, X. Zhang, X. Li, S. Liu, Y. Zhang and J. Xu, *J. Phys. Chem. C*, 2011, **115**, 17574; (c) J. Huang, N. Sun, P. Chen, R. Tang, Q. Li, D. Ma and Z. Li, *Chem. Commun.*, 2014, **50**, 2136; (d) J. Huang, N. Sun, Y. Dong, R. Tang, P. Lu, P. Cai, Q. Li, D. Ma, J. Qin and Z. Li, *Adv. Funct. Mater.*, 2013, **23**, 2329; (e) R. Misra, T. Jadhav, B. Dhokale and S. M. Mobin, *Chem. Commun.*, 2014, **50**, 9076.
- (a) C. P. Ma, B. J. Xu, G. Y. Xie, J. J. He, X. Zhou, B. Y. Peng, L. Jiang, B. Xu, W. J. Tian, Z. G. Chi, S. W. Liu, Y. Zhang and J. R. Xu, *Chem. Commun.*, 2014, **50**, 7374; (b) N. Zhao, J. W. Y. Lam, H. H. Y. Sung, N. Xie, S. Chen, H. Su, M. Gao, I. D. Williams, K. S. Wong and B. Z. Tang, *Chem. Commun.*, 2012, **48**, 8637.
- B. Maleki and H. Salehabadi, *Eur. J. Chem.*, 2010, **1**, 377380.
- J. Huang, X. Yang, J. Wang, C. Zhong, L. Wang, J. Qin and Z. Li, *J. Mater. Chem.*, 2012, **22**, 2478.
- J. D. Luo, Z. L. Xie, J. W. Y. Lam, L. Cheng, H. Y. Chen, C. F. Qiu, H. S. Kwok, X. W. Zhan, Y. Q. Liu, D. B. Zhu and B. Z. Tang, *Chem. Commun.*, 2001, 1740.
- B. Z. Tang, Y. Geng, J. W. Y. Lam, B. Li, X. Jing, X. Wang, F. Wang, A. B. Pakhomov and X. Zhang, *Chem. Mater.*, 1999, **11**, 1581.
- (a) M. J. Frisch, G. W. Trucks, H. B. Schlegel, G. E. Scuseria, M. A. Robb, J. R. Cheeseman, G. Scalmani, V. Barone, B. Mennucci, G. A. Petersson, H. Nakatsuji, M. Caricato, X. Li, H. P. Hratchian, A. F. Izmaylov, J. Bloino, G. Zheng, J. L. Sonnenberg, M. Hada, M. Ehara, K. Toyota, R. Fukuda, J. Hasegawa, M. Ishida, T. Nakajima, Y. Honda, O. Kitao, H. Nakai, T. Vreven, J. A. Montgomery Jr, J. E. Peralta, F. Ogliaro, M. Bearpark, J. J. Heyd, E. Brothers, K. N. Kudin, V. N. Staroverov, R. Kobayashi, J. Normand, K. Raghavachari, A. Rendell, J. C. Burant, S. S. Iyengar, J. Tomasi, M. Cossi, N. Rega, N. J. Millam, M. Klene, J. E. Knox, J. B. Cross, V. Bakken, C. Adamo, J. Jaramillo, R. Gomperts, R. E. Stratmann, O. Yazyev, A. J. Austin, R. Cammi, C. Pomelli, J. W. Ochterski, R. L. Martin, K. Morokuma, V. G. Zakrzewski, G. A. Voth, P. Salvador, J. J. Dannenberg, S. Dapprich, A. D. Daniels, O. Farkas, J. B. Foresman, J. V. Ortiz, J. Cioslowski and D. J. Fox, *Gaussian 09, revision A.02*, Gaussian, Inc., Wallingford, CT, 2009; (b) C. Lee, W. Yang and R. G. Parr, *Phys. Rev. B: Condens. Matter Mater. Phys.*, 1988, **37**, 785; (c) A. D. J. Becke, *Chem. Phys.*, 1993, **98**, 1372.